Completion of lunar magma ocean solidification at 4.43 Ga

Nicolas Dauphas[a,1] (iD), Zhe J. Zhang[a], Xi Chen[a] (iD), Mélanie Barboni[b], Dawid Szymanowski[c,d] (iD), Blair Schoene[d], Ingo Leya[e], and Kevin D. McKeegan[f] (iD)

Crystallization of the lunar magma ocean yielded a chemically unique liquid residuum named KREEP. This component is expressed as a large patch on the near side of the Moon and a possible smaller patch in the northwest portion of the Moon's South Pole-Aitken basin on the far side. Thermal models estimate that the crystallization of the lunar magma ocean (LMO) could have spanned from 10 and 200 My, while studies of radioactive decay systems have yielded inconsistent ages for the completion of LMO crystallization covering over 160 My. Here, we show that the Moon achieved >99% crystallization at 4,429 ± 76 Ma, indicating a lunar formation age of ~4,450 Ma or possibly older. Using the ^{176}Lu–^{176}Hf decay system ($t_{1/2}$ = 37 Gy), we found that the initial $^{176}Hf/^{177}Hf$ ratios of lunar zircons with varied U–Pb ages are consistent with their crystallization from a KREEP-rich reservoir with a consistently low $^{176}Lu/^{177}Hf$ ratio of 0.0167 that emerged ~140 My after solar system formation. The previously proposed younger model age of ~4.33 Ga for the source of mare basalts (240 My after solar system formation) might reflect the timing of a large impact. Our results demonstrate that lunar magma ocean crystallization took place while the Moon was still battered by planetary embryos and planetesimals leftover from the main stage of planetary accretion. The study of Lu–Hf model ages for samples brought back from the South Pole-Aitken basin will help to assess the lateral continuity of KREEP and further understand its significance in the early history of the Moon.

Moon | zircon | age | KREEP

The mode and pace of Earth's growth are topics of considerable discussion, with two endmember theories involving fast accretion of small pebbles (1) or protracted accretion of large embryos thousands of kilometers in size (2). Where all models agree is that late in its history, the proto-Earth experienced one or several collisions with large planetary objects. One such impactor named Theia is speculated to have produced the Moon (3–5). Despite sustained efforts over decades to study samples brought back from the Moon by the Apollo, Luna, and Chang'E 5 missions, there is still considerable uncertainty on when the giant Moon-forming impact occurred (6–13). This impact could have been the last globally sterilizing event, and Earth might have been continuously habitable since then or shortly thereafter (14).

Geochemical evidence indicates that the Moon went through a magma ocean stage, whereby most or all of it was molten (15). Its cooling was associated with crystallization of a series of minerals with distinctive compositions, which drove the residual liquid to evolve chemically toward a composition called KREEP that is enriched in highly incompatible elements, notably potassium (K), rare earth elements (REEs), and phosphorus (P). KREEP was discovered in basalts recovered by the Apollo mission (15), and it was later detected remotely through γ-ray spectroscopy as two large patches of K and Th-enriched rocks positioned antipodally on the Moon in the Procellarum KREEP Terrane (PKT) and the South Pole-Aitken Terrane (SPAT) (16–20). Several strategies have been devised to date the formation of the KREEP reservoir, but no consensus has been reached on its age, with values spanning 160 My from 4.51 to 4.35 Ga (6–11). A robust age for KREEP would provide a minimum age for the Moon-forming impact.

The ^{176}Lu–^{176}Hf decay system [$t_{1/2}$ = 37 Gy (21, 22)] can be used to date the end of lunar magma ocean crystallization (7, 23–25). Application of this tool relies on the fact that during differentiation of the lunar magma ocean, Lu was preferentially retained in the mantle, while the crust and the residual melt layer known as KREEP became relatively enriched in Hf. As a result, once KREEP formed, its $^{176}Hf/^{177}Hf$ ratio increased more slowly than the bulk Moon, which is assumed to be like chondritic meteorites (CHUR = Chondritic Uniform Reservoir) (26) because both Lu and Hf are refractory lithophile elements. By analyzing the isotopic compositions of bulk rocks and zircon minerals, one can determine when KREEP evolved as an isolated reservoir from CHUR and thus date KREEP formation. Since KREEP is thought to have formed when the lunar magma

Significance

The Moon started as a fully molten body that gradually separated into layers as it cooled and crystallized. After 99% of the lunar magma ocean solidified, a unique residual liquid called KREEP, enriched in potassium (K), rare earth elements (REE), and phosphorus (P), was formed. Our study indicates that this KREEP liquid formed 4,429 ± 76 Mya, approximately 140 My after the solar system's birth. We also found that the KREEP liquid, as sampled by the Apollo missions, was remarkably uniform. Further studies of samples from the South Pole-Aitken basin will help clarify whether this uniformity extends laterally from the nearside to the farside of the Moon.

Author affiliations: [a]Origins Laboratory, Department of the Geophysical Sciences and Enrico Fermi Institute, The University of Chicago, Chicago, IL 60637; [b]School of Earth and Space Exploration, Arizona State University, Tempe, AZ 85281; [c]Institute of Geochemistry and Petrology, ETH Zurich, Zurich 8092, Switzerland; [d]Department of Geosciences, Princeton University, Princeton, NJ 08544; [e]Space Sciences and Planetology, University of Bern, Bern 3012, Switzerland; and [f]Department of Earth, Planetary, and Space Sciences, University of California, Los Angeles, CA 90095

ocean (LMO) was 99% crystallized (27), dating the formation of this reservoir is equivalent to determining when LMO crystallization was nearly complete. Bulk rocks have been used for that purpose, but these samples formed relatively late, requiring large extrapolation of the KREEP value backward in time, which can lead to highly uncertain age estimates (23). A more robust approach is to measure the initial ^{176}Hf/^{177}Hf (or ε^{176}Hf; the relative departure in parts per 10^4 from the CHUR ratio) of zircons that crystallized from lunar rocks containing a large KREEP component (7, 24, 25). Zircons are chemically resistant and have low Lu/Hf ratios, and their ages can be precisely determined using U–Pb geochronology, so they represent ideal time capsules to track the temporal evolution of ε^{176}Hf in the KREEP reservoir.

Taylor et al. (25) and Barboni et al. (7) analyzed lunar zircons using different methodologies (*SI Appendix*, Fig. S4). While these studies provide valuable insights, their Lu–Hf data had significant uncertainties due to the use of peak stripping to correct for isobaric interferences during data reduction. To better define the age of KREEP, we have measured a new set of lunar zircons using improved methodologies (24) (see *SI Appendix* for details). These advances include separating Hf from elements that can cause isobaric interferences and accounting for the effect of Lu/Hf fractionation during sample processing. We have measured U/Pb ages, Hf isotopic compositions, and Lu/Hf ratios in lunar zircon leachates and residues treated by chemical abrasion intended to remove zircon domains more susceptible to Pb-loss or gain (24). The U/Pb ages were measured by isotope-dilution thermal ionization mass spectrometry at Princeton University. Hafnium from the same solutions were purified from interfering and all matrix elements, including Zr, for Hf isotopic analysis by MC-ICP-MS at the University of Chicago (24). The ^{176}Hf/^{177}Hf ratios were corrected for ^{176}Lu-decay using measured Lu/Hf ratios and U-Pb ages, as well as for neutron capture effects associated with exposure to cosmic rays, using ε^{178}Hf and ε^{180}Hf as neutron dosimeters (23, 24) (*SI Appendix*, Eq. **S2**). Some U–Pb ages and Hf isotopic analyses were previously reported, showing that a significant fraction of zircons crystallized in a short period of time starting at 4.338 Ga; a date that could correspond to the South Pole-Aitken impact (28). Indeed, this impact may have been powerful enough to cause the antipodal excavation of KREEP in the PKT (29). The full collection of zircons that we analyzed span 3.94 to 4.34 Ga in crystallization age, allowing us to constrain the age of KREEP and to evaluate the homogeneity of the Lu/Hf ratio in this reservoir. A potential difficulty with coupled U–Pb and Lu–Hf analyses of zircons is that Pb loss can occur without initial ε^{176}Hf resetting. This can be remediated by chemical abrasion, which selectively removes domains susceptible to Pb loss, preserving closed-system domains that yield more concordant U–Pb ages (7, 24, 30). Most of our U–Pb ages are near-concordant and we found consistent ^{206}Pb-^{207}Pb ages between the different aliquots (L2 and R), indicating that the ages are most likely reliable (28), especially over the time span that we are interested in. The chemical abrasion procedure may introduce artifacts, most notably through the fractionation of the Lu/Hf ratio during dissolution if insoluble, Lu-rich fluorides precipitate (31). This could affect the correction of ε^{176}Hf for in situ ^{176}Lu decay since zircon crystallization.

We measured a total of 36 zircon grains, and for many of these, we measured several fractions, corresponding to a total of 62 Lu–Hf and U–Pb analyses (*SI Appendix*, Table S1 and Dataset S1). A fraction of these were previously published to test the technique (24) and better understand the origin of the 4.338 Ga peak in the age distribution of lunar zircons (28). To evaluate the reliability of the data, we compare data for leachates and residues of

chemical abrasion (24). For each zircon, three fractions were recovered during chemical abrasion. Leachate 1 (L1) was recovered after leaching with 90 µL 29 M HF for 6 h at 180 °C. Leachate 2 (L2) was recovered after further processing the zircon through the same dissolution procedure. The residue (R) was finally dissolved in a Parr bomb using 90 µL 29 M HF for 60 h at 210 °C. The first leachate was not used because it is prone to disturbance and contamination by common (nonradiogenic) Pb.

Our data are considered most reliable when L2 and R display similar ages and initial ε^{176}Hf values, as this indicates that the zircon has a straightforward history and that laboratory processing has not altered the intrinsic composition of the zircon (see *SI Appendix* for detail). Indeed, any episode of partial Pb-loss or gain would have likely affected U–Pb ages of L2 and R differently, and any problem with data accuracy, correction of cosmogenic effects, or fractionation of Lu/Hf ratio during zircon dissolution would have resulted in different initial ε^{176}Hf for L2 and R. The zircon measurements that yield consistent values between L2 and R are part of what we call *Tier 1*. There are 16 data points (initial ε^{176}Hf-U/Pb age) in this subset.

In most instances where the initial corrected ε^{176}Hf values differ between L2 and R, the raw ε^{176}Hf values agree. This discrepancy is often due to significant and varying Lu/Hf ratios (*SI Appendix*, Fig. S2). It is highly unlikely for different domains within a single zircon to have originated with distinct initial ε^{176}Hf values and Lu/Hf ratios, and then fortuitously converge to similar present-day ε^{176}Hf values after ^{176}Lu decay. The different initial corrected ε^{176}Hf values are most likely an analytical artifact from fractionation of the Lu/Hf during processing. The residues (R) hold the majority of Lu and Hf and are therefore more reliable than L2. The subset of data that comprises all residue measurements (R) together with L2 measurements when they agree with R (*Tier 1* above) is called *Tier 3*. There are 40 data points in this subset. We also defined a *Tier 2* dataset comprising 26 data points that are intermediate in terms of reliability between the *Tier 1* and *Tier 3* datasets. The results are consistent with the other datasets and they are only discussed in *SI Appendix*. Insoluble fluoride may be causing discrepancies between L2 and R in some samples. After leaching, we pipette out the leachate and rinse the residue multiple times with different acids, pipetting out each time. We then place the zircon residue back on the hotplate in 6 M HCl for at least 6 h, followed by additional rinses with various acids. This process aims to dissolve fluorides; however, it may not have been fully effective. Further work will be necessary to assess if this an issue and to develop a mitigation strategy to achieve a higher proportion of *Tier 1* data.

The relationships between the ε^{176}Hf initial values and Pb–Pb ages are plotted in Fig. 1 for *Tiers 1* and *3* zircon datasets. The data can be fit with a single line (the reduced-χ^2 also known as mean square weighted deviation MSWD are 0.85 and 1.3 for *Tiers 1* and *3* datasets with $n - 2 = 16$ and 38 degrees of freedom, respectively; the 2.5 to 97.5% interquantile range for the reduced-χ^2 distribution for those degrees of freedom are 0.43 to 1.80 and 0.60 to 1.50), and are therefore consistent with all zircons crystallizing at different times from a melt of uniform Hf isotopic composition. The intercepts between the best-fit lines and the x-axes give model ages for KREEP of 4,429 ± 76 Ma (±95% c.i.) and 4,450 ± 77 (±95% c.i.) My for *Tiers 1* and *3*, respectively. The slopes of the ε^{176}Hf-age regressions correspond to ^{176}Lu/^{177}Hf ratios of 0.0167 ± 0.0022 (±95% c.i.) and 0.0172 ± 0.0016 (±95% c.i.) for *Tiers 1* and *3*, respectively (*SI Appendix*, Eq. **S10**). There is good agreement between all tiers of data quality, indicating that the results are not influenced by our parsing in tiers. We use *Tier 1* results for discussion as they are identical within error with *Tier 3* but are less likely to be affected by any form of bias.
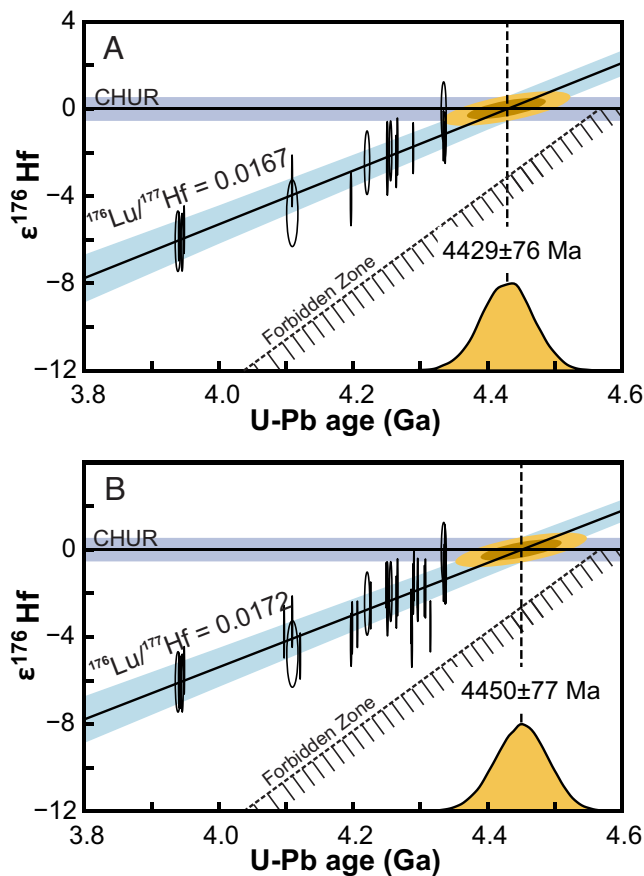
Fig. 1. Calculation of the ^{176}Lu–^{176}Hf model age of KREEP magma formation based on lunar zircon $\varepsilon^{176}Hf$ and U–Pb data (*SI Appendix*, Table S1 and Dataset S1). Panels (*A* and *B*) show the results for different tiers of data quality. *Tier 1* (*A*) corresponds to data where $\varepsilon^{176}Hf$ values are consistent between leachate 2 (L2) and residue (R) of the chemical abrasion procedure, ensuring that the data are of the upmost quality (*n* = 16). *Tier 3* (*B*) comprises all R measurements, together with L2 measurements when they agree with R (*n* = 51). We focus on high-quality *Tier 1* data (*A*), but all tiers (including intermediate *Tier 2*; see *SI Appendix*) yield model ages and Lu/Hf ratios for KREEP that are identical within error. All data can be fit with a single line (MSWD = 0.85 for *Tier 1*), consistent with isolation of KREEP at a well-defined time (4,429 ± 76 Ma; the 68 and 95% confidence ellipses for the intercept with CHUR are shown in brown and yellow) and crystallization of the zircons at different times from melts of uniform $^{176}Lu/^{177}Hf$ (0.0167 ± 0.0022). (±95% c.i.). The model age is given by the intercept between the best-fit line (solid black line with light blue 95% c.i.) and CHUR (horizontal black solid line with dark blue 95% c.i.). The $^{176}Lu/^{177}Hf$ ratio of KREEP is given by the slope of the best-fit line (*SI Appendix*, Eq. **S10**). The forbidden zone (hatched) corresponds to the minimum obtainable $\varepsilon^{176}Hf$ value for a hypothetical reservoir formed at the formation of the solar system with $^{176}Lu/^{177}Hf=0$. The yellow curve on the x-axis is the marginal probability distribution for the model age of KREEP (the joint probability distribution is shown as an ellipse). All errors are 95% c.i. The $\varepsilon^{176}Hf$ values shown here were corrected for cosmogenic effects using $\varepsilon^{178}Hf$ (23, 24). Correcting these effects using $\varepsilon^{180}Hf$ yields more scattered $\varepsilon^{176}Hf$ values and more uncertain fit parameters (KREEP age= 4,448±81 Ma, $^{176}Lu/^{177}Hf$ = 0.0162 ± 0.0026 for *Tier 1*) that still overlap within error with $\varepsilon^{178}Hf$-corrected data (*SI Appendix*, Fig. S7).

The $^{176}Lu/^{177}Hf$ ratio of KREEP inferred here is consistent but more precise than prior estimates obtained by measuring the trace element composition of KREEP-enriched rocks returned from the Moon by the Apollo mission, which gave ratios of 0.0164 (25), 0.0154 ± 0.0034 (23), and 0.00153 ± 0.0033 (32). This supports the view that zircons indeed crystallized from a relatively uniform KREEP reservoir. Taylor et al. (25) analyzed zircon grains in situ using secondary ion mass spectrometry for U–Pb and laser ablation multicollector inductively coupled plasma mass spectrometry (LA-MC-ICP-MS) for Lu–Hf and found significant scatter in the data beyond individual data uncertainty (*SI Appendix*,

Fig. S4), with a peak in the model age distribution at ~4.48 Ga. Barboni et al. (7) also found significant scatter (*SI Appendix*, Fig. S4) with model age estimates for individual zircons that largely overlap with ours, but with a few data points giving older model ages. The most critical data that give older ages have large uncertainties, on which the present study improves. The present Hf isotopic data have higher precision, and their accuracy is improved through purification of Hf by chromatography.

Borg and Carlson (9) made a case for crystallization of much of the lunar magma ocean at 4.33 Ga, with the strongest piece of evidence provided by ^{146}Sm–^{142}Nd ($t_{1/2}$ = 103 My) and ^{147}Sm–^{143}Nd ($t_{1/2}$ = 106 Gy) systematics applied to the source of mare basalts. We have reexamined the dataset of Borg et al. (8) and agree with their assessment that a model age of lunar magma ocean differentiation of 4.44 Ga provides a poorer fit to initial $^{142}Nd/^{144}Nd$ ratios of mare basalts compared to a model age of 4.33 Ga (*SI Appendix*, Fig. S5), but in both cases, there is significant scatter with 5 out of 30 samples that cannot be explained. A difficulty with the interpretation of LMO crystallization at 4.33 Ga is that single lunar zircon mineral grains have been dated at 4.42 Ga (6), contradicting the view that LMO differentiation occurred late. Older zircon grains have also been found on Earth (33, 34). Interestingly, the 4.33 Ga age inferred for the source of the mare basalts also corresponds to a marked and narrow peak (~4 My duration) in the age distribution of U–Pb zircon ages, which Barboni et al. (28) interpreted to correspond to large scale melting induced by a large impact, possibly associated with the formation of the South Pole-Aitken basin. Even if such an impact did not induce complete melting of the ultramafic cumulate that is thought to be the main source of the mare basalts, it might have induced melting of the most fusible components of the cumulate (35), allowing Sm and Nd redistribution and equilibration through reactive melt infiltration (36). It could have also induced mixing and subsequent density separation of minerals within the Moon (37). Both factors could have contributed to resetting Sm–Nd systematics at a bulk rock scale, so the Sm–Nd model age may date a late-stage large impact rather than early crystallization of the lunar magma ocean.

We obtain an age for separation of KREEP of 4,429 ± 76 Ma (Fig. 1). The oldest zircon that we have analyzed here is 4,338 Ma, but previous studies have reported older single mineral ages that overlap with our KREEP model age. Nemchin et al. (6) reported an age of 4,417 ± 6 Ma in a zircon from a lunar breccia using an in situ technique. Zhang et al. (10) also reported an age of 4,460 ± 30 Ma in a zircon. The authors originally dismissed the data because applying another technique on the same zircon yielded an age 300 Ma younger. However, Greer et al. (11) found no evidence for secondary disturbance in this zircon and argued that the older age was real. Old ages (>4.4 Ga) were also reported for some ferroan anorthosites (38–41) that are thought to represent flotation of a plagioclase crust during LMO crystallization. These older ages were dismissed due to the lack of concordance among different radiochronometers and disagreement with more recent data (9). Borg and Carlson (9) argued that the formation of the ferroan anorthosite suite was most reliably dated using Sm–Nd systematics applied to Apollo samples 60025 (37), 62237 (42), and Y-86032 (39), with sample 60025 yielding the most precise age estimate of 4.367 ± 0.011 Ga. However, the Sm–Nd crystallization ages obtained from this sample do not all agree, as Carlson and Lugmair (40) reported a notably older age of 4.44 ± 0.02 Ga. Establishing the concordance with Pb–Pb ages is challenging, given that plagioclase and pyroxene yield disparate ages in this sample (37, 43). Sample 60025 is a polymict breccia containing materials not all derived

from the LMO (44). The age discrepancy may therefore stem from differences in the analyzed materials, with the older age of 4.44 ± 0.02 Ga (40) potentially representing the formation of a flotation crust.

The Lu–Hf model age of KREEP formation corresponds to the time when the LMO reached 99 to 99.9% crystallization (*SI Appendix,* Fig. S6) (27). The age of KREEP therefore gives a minimum age for the Moon. To go beyond this and provide a solid constraint on the time of the giant impact, one must rely on uncertain models of lunar magma ocean cooling. A few thousands of years is all it took for the lunar magma ocean to cool to 80% crystallization (45). What happened beyond this is uncertain. The formation of a plagioclase flotation crust likely hampered further heat loss. In addition, some heat was deposited inside the Moon by tidal dissipation (45–49). Models involving a simple stagnant conductive lid predict a cooling time of 10 to 30 My (45), meaning that the Moon could have formed 4,449 ± 76 Mya. Interestingly, this is close to the age of 4.44 ± 0.02 Ga obtained for ferroan anorthosite 60025 by Carlson and Lugmair (40), possibly dating the formation of a flotation crust. However, some models using low thermal conductivity for the anorthositic crust and considering extraction of melt from mafic cumulate predict a crystallization time of 200 My (46). Our results on the age of KREEP show that such a prolonged crystallization time is unlikely because it would put lunar formation before solar system formation, but a 150 My cooling time would agree with current knowledge. It has been argued, based on ^{182}Hf–^{182}W systematics, that the Moon could have formed 40 to 74 My after the birth of the solar system (4.53 to 4.49 Ga) (50, 51). However, this age may lack significance if the ^{182}W excess in lunar rocks relative to terrestrial rocks is due to disproportionate late accretion of meteoritic material after core formation rather than ^{182}Hf-decay (13). Taken at face value, such an age for lunar formation would mean that the LMO took ~60 My to be fully solidified.

This study shows that zircons recovered from the Moon by the Apollo missions were all derived from a single KREEP reservoir

that was isolated from the bulk silicate Moon at 4.43 Ga. Remote sensing γ-ray mapping of K and Th on the Moon has revealed the extent of the Procellarum KREEP Terrane (18, 52) that is likely the predominant chemical source of the lunar zircons found in rocks from the Apollo missions. The same mapping showed that a smaller patch of material enriched in KREEP is also present in the South Pole-Aitken terrane, on the antipode of the Procellarum KREEP Terrane (19, 20). The Chang'e 6 mission retrieved rocks from the South Pole-Aitken basin. If zircons are found in these rocks, they should have experienced a different impact history than those from the Apollo missions, with the South Pole-Aitken impact expected to be featured predominantly in their age distribution. If KREEP was a uniform layer, which is the prevailing view, we expect that those zircons will plot on the same $\varepsilon^{176}Hf$-age trend as the one established here, regardless of differences in their age distribution. However, the alternative that KREEP, which formed when the Moon was 99% crystallized, was in fact composed of pools of magmas isolated at different times cannot be excluded. As we enter a new era of Moon exploration and sampling, our determination of the age of KREEP serves as a fundamental reference for testing hypotheses regarding its nature and occurrence within the South Pole-Aitken basin.

Data, Materials, and Software Availability. All study data are included in the article and/or supporting information.

1. A. Johansen *et al.*, A pebble accretion model for the formation of the terrestrial planets in the Solar System. *Sci. Adv.* **7**, eabc0444 (2021).
2. J. Chambers, G. Wetherill, Making the terrestrial planets: N-body integrations of planetary embryos in three dimensions. *Icarus* **136**, 304–327 (1998).
3. W. K. Hartmann, D. R. Davis, Satellite-sized planetesimals and lunar origin. *Icarus* **24**, 504–515 (1975).
4. A. G. W. Cameron, W. R. Ward, The origin of the Moon. *Lunar Planet. Sci. Conf.* **7**, 120 (1976).
5. R. M. Canup *et al.*, Origin of the Moon. *Rev. Mineral. Geochem.* **89**, 53–102 (2023).
6. A. Nemchin *et al.*, Timing of crystallization of the lunar magma ocean constrained by the oldest zircon. *Nat. Geosci.* **2**, 133–136 (2009).
7. M. Barboni *et al.*, Early formation of the Moon 4.51 billion years ago. *Sci. Adv.* **3**, e1602365 (2017).
8. L. E. Borg *et al.*, Isotopic evidence for a young lunar magma ocean. *Earth Planet. Sci. Lett.* **523**, 115706 (2019).
9. L. E. Borg, R. W. Carlson, The evolving chronology of Moon formation. *Annu. Rev. Earth Planet. Sci.* **51**, 25–52 (2023).
10. B. Zhang *et al.*, Radiogenic Pb mobilization induced by shock metamorphism of zircons in the Apollo 72255 Civet Cat norite clast. *Geochim. Cosmochim. Acta* **302**, 175–192 (2021).
11. J. Greer *et al.*, 4.46 Ga zircons anchor chronology of lunar magma ocean. *Geochem. Perspect. Lett.* **27**, 49–53 (2023).
12. M. M. Thiemens, P. Sprung, R. O. Fonseca, F. P. Leitzke, C. Münker, Early Moon formation inferred from hafnium–tungsten systematics. *Nat. Geosci.* **12**, 696–700 (2019).
13. T. S. Kruijer, G. J. Archer, T. Kleine, No ^{182}W evidence for early Moon formation. *Nat. Geosci.* **14**, 714–715 (2021).
14. R. I. Citron, S. T. Stewart, Large impacts onto the early Earth: Planetary sterilization and iron delivery. *Planet. Sci. J.* **3**, 116 (2022).
15. P. H. Warren, The magma ocean concept and lunar evolution. *Annu. Rev. Earth Planet. Sci.* **13**, 201–240 (1985).
16. D. Lawrence *et al.*, Small-area thorium features on the lunar surface. *J. Geophys. Res.: Planets* **108**, 5102 (2003).
17. T. H. Prettyman *et al.*, Elemental composition of the lunar surface: Analysis of gamma ray spectroscopy data from Lunar Prospector. *J. Geophys. Res.: Planets* **111**, E12007 (2006).
18. S. Kobayashi *et al.*, Lunar farside Th distribution measured by Kaguya gamma-ray spectrometer. *Earth Planet. Sci. Lett.* **337**, 10–16 (2012).
19. M. Naito *et al.*, Potassium and thorium abundances at the South Pole-Aitken basin obtained by the Kaguya gamma-ray spectrometer. *J. Geophys. Res.: Planets* **124**, 2347–2358 (2019).
20. J. J. Hagerty, D. Lawrence, B. Hawke, Thorium abundances of basalt ponds in South Pole-Aitken basin: Insights into the composition and evolution of the far side lunar mantle. *J. Geophys. Res.: Planets* **116**, E06001 (2011).

21. U. Söderlund, P. J. Patchett, J. D. Vervoort, C. E. Isachsen, The ^{176}Lu decay constant determined by Lu-Hf and U-Pb isotope systematics of Precambrian mafic intrusions. *Earth Planet. Sci. Lett.* **219**, 311–324 (2004).
22. T. Hayakawa, T. Shizuma, T. Iizuka, Half-life of the nuclear cosmochronometer ^{176}Lu measured with a windowless 4π solid angle scintillation detector. *Commun. Phys.* **6**, 299 (2023).
23. P. Sprung, T. Kleine, E. E. Scherer, Isotopic evidence for chondritic Lu/Hf and Sm/Nd of the Moon. *Earth Planet. Sci. Lett.* **380**, 77–87 (2013).
24. X. Chen *et al.*, Methodologies for ^{176}Lu–^{176}Hf analysis of Zircon grains from the Moon and beyond. *ACS Earth Space Chem.* **8**, 36–53 (2023), 10.1021/acsearthspacechem.3c00093.
25. D. J. Taylor, K. D. McKeegan, T. M. Harrison, Lu-Hf zircon evidence for rapid lunar differentiation. *Earth Planet. Sci. Lett.* **279**, 157–164 (2009).
26. A. Bouvier, J. D. Vervoort, P. J. Patchett, The Lu-Hf and Sm-Nd isotopic composition of CHUR: Constraints from unequilibrated chondrites and implications for the bulk composition of terrestrial planets. *Earth Planet. Sci. Lett.* **273**, 48–57 (2008).
27. P. H. Warren, J. T. Wasson, The origin of KREEP. *Rev. Geophys.* **17**, 73–88 (1979).
28. M. Barboni *et al.*, High precision U-Pb zircon dating identifies a major magmatic event on the Moon at 4.338 Ga. *Sci. Adv.* **10**, eadn9871 (2024).
29. M. J. Jones *et al.*, A South Pole-Aitken impact origin of the lunar compositional asymmetry. *Sci. Adv.* **8**, eabm8475 (2022).
30. J. M. Mattinson, Zircon U-Pb chemical abrasion ("CA-TIMS") method: Combined annealing and multi-step partial dissolution analysis for improved precision and accuracy of zircon ages. *Chem. Geol.* **220**, 47–66 (2005).
31. J. Blichert-Toft, F. Albarède, The Lu-Hf isotope geochemistry of chondrites and the evolution of the mantle-crust system. *Earth Planet. Sci. Lett.* **148**, 243–258 (1997).
32. A. M. Gaffney, L. E. Borg, A young solidification age for the lunar magma ocean. *Geochim. Cosmochim. Acta* **140**, 227–240 (2014).
33. S. A. Wilde, J. W. Valley, W. H. Peck, C. M. Graham, Evidence from detrital zircons for the existence of continental crust and oceans on the Earth 4.4 Gyr ago. *Nature* **409**, 175–178 (2001).
34. P. Holden *et al.*, Mass-spectrometric mining of Hadean zircons by automated SHRIMP multi-collector and single-collector U/Pb zircon age dating: The first 100,000 grains. *Int. J. Mass Spectrom.* **286**, 53–63 (2009).
35. C. L. McLeod, A. D. Brandon, R. M. Armytage, Constraints on the formation age and evolution of the Moon from ^{142}Nd–^{143}Nd systematics of Apollo 12 basalts. *Earth Planet. Sci. Lett.* **396**, 179–189 (2014).
36. G. Borghini *et al.*, Fast REE re-distribution in mantle clinopyroxene via reactive melt infiltration. *Geochem. Perspect. Lett.* **26**, 40–44 (2023).
37. L. E. Borg, J. N. Connelly, M. Boyet, R. W. Carlson, Chronological evidence that the Moon is either young or did not have a global magma ocean. *Nature* **477**, 70–72 (2011).

38. M. D. Norman, L. E. Borg, L. E. Nyquist, D. D. Bogard, Chronology, geochemistry, and petrology of a ferroan noritic anorthosite clast from Descartes breccia 67215: Clues to the age, origin, structure, and impact history of the lunar crust. *Meteorit. Planet. Sci.* **38**, 645–661 (2003).

39. L. Nyquist *et al.*, Feldspathic clasts in Yamato-86032: Remnants of the lunar crust with implications for its formation and impact history. *Geochim. Cosmochim. Acta* **70**, 5990–6015 (2006).

40. R. W. Carlson, G. W. Lugmair, The age of ferroan anorthosite 60025: Oldest crust on a young Moon? *Earth Planet. Sci. Lett.* **90**, 119–130 (1988).

41. C. Alibert, M. D. Norman, M. T. McCulloch, An ancient Sm-Nd age for a ferroan noritic anorthosite clast from lunar breccia 67016. *Geochim. Cosmochim. Acta* **58**, 2921–2926 (1994).

42. C. Sio, L. Borg, W. Cassata, The timing of lunar solidification and mantle overturn recorded in ferroan anorthosite 62237. *Earth Planet. Sci. Lett.* **538**, 116219 (2020).

43. B. Hanan, G. Tilton, 60025: Relict of primitive lunar crust? *Earth Planet. Sci. Lett.* **84**, 15–21 (1987).

44. M. Torcivia, C. Neal, Unraveling the components within Apollo 16 ferroan anorthosite suite cataclastic anorthosite sample 60025: Implications for the lunar magma ocean model. *J. Geophys. Res.: Planets* **127**, e2020JE006799 (2022).

45. L. T. Elkins-Tanton, S. Burgess, Q.-Z. Yin, The lunar magma ocean: Reconciling the solidification process with lunar petrology and geochronology. *Earth Planet. Sci. Lett.* **304**, 326–336 (2011).

46. M. Maurice, N. Tosi, S. Schwinger, D. Breuer, T. Kleine, A long-lived magma ocean on a young Moon. *Sci. Adv.* **6**, eaba8949 (2020).

47. V. Perera, A. P. Jackson, L. T. Elkins-Tanton, E. Asphaug, Effect of reimpacting debris on the solidification of the lunar magma ocean. *J. Geophys. Res.: Planets* **123**, 1168–1191 (2018).

48. J. Meyer, L. Elkins-Tanton, J. Wisdom, Coupled thermal–orbital evolution of the early Moon. *Icarus* **208**, 1–10 (2010).

49. Z. Tian, J. Wisdom, L. Elkins-Tanton, Coupled orbital-thermal evolution of the early Earth-Moon system with a fast-spinning Earth. *Icarus* **281**, 90–102 (2017).

50. M. M. Thiemens *et al.*, Reply to: No ^{182}W evidence for early Moon formation. *Nat. Geosci.* **14**, 716–718 (2021).

51. M. M. Thiemens, P. Sprung, R. O. C. Fonseca, F. P. Leitzke, C. Münker, Early Moon formation inferred from hafnium–tungsten systematics. *Nat. Geosci.* **12**, 696–700 (2019).

52. D. Lawrence *et al.*, Global elemental maps of the Moon: The Lunar Prospector gamma-ray spectrometer. *Science* **281**, 1484–1489 (1998).